Liquid-liquid phase separation in cylindrical pores: Quench molecular dynamics and Monte Carlo simulations

Lev D. Gelb and K. E. Gubbins
School of Chemical Engineering, Olin Hall, Cornell University, Ithaca, New York 14853-5201
(Received 20 March 1997)

We have studied the liquid-liquid phase separation of a binary mixture confined in three different cylindrical pores by several simulation methods. The phase diagrams of the fluid mixture in the three pores were determined using histogram-biased semigrand Monte Carlo simulations, and the kinetics of phase separation of the confined liquid mixture were studied using quench molecular dynamics. In these systems, the interactions between the two fluids and the pore wall are identical so that no wetting occurs and the fluid separates into a series of pluglike domains after a temperature quench. We have determined that the growth of these domains is given by a power law for systems near to their critical temperature, while for deeper quenches it proceeds by a power law at short times which crosses over to a slower growth when the plug-shaped domains are large enough to completely block the pore. Domains in these systems are shown to grow by a condensation mechanism. Using a simple thermodynamic model we analyze the $P(X)$ probability distributions from our Monte Carlo simulations, and estimate the equilibrium domain lengths in two pores over a range of temperature. These lengths are larger than those reached in our molecular dynamics simulations. In order to assess these estimations, we have performed very long canonical Monte Carlo simulations to directly determine the equilibrium domain lengths in a few of these pores. [S1063-651X(97)00709-5]

PACS number(s): 64.70.Ja, 47.55.Mh, 61.20.Ja, 64.75.+g

I. INTRODUCTION

When fluid mixtures are confined in very small spaces their behavior is quite different than in the bulk phase. The liquid-liquid miscibility phase diagram for an adsorbed mixture can be very different from that of its bulk counterpart, and in sufficiently small spaces the liquid-liquid transition can be suppressed entirely. Since microporous membranes and adsorbates are routinely used in industrial separations processes, understanding these effects is important in developing new separations technologies.

Microporous systems are difficult to study experimentally because the pore structures of most of the commonly used membranes and adsorbates are quite complex and difficult to determine, so that these materials are not well characterized at the molecular level. Furthermore, many common adsorbents have amorphous structures with broad distributions of pore sizes and shapes, which makes a microscopic understanding of fluid behavior in these systems very difficult.

In addition to strongly affecting the liquid-liquid coexistence curve, confinement in small pores changes the kinetics of liquid-liquid phase separation. Many studies indicate that in quenching experiments these systems rarely achieve macroscopic phase separation and instead become ''frozen'' into partially phase-separated states, with many small domains of each phase that are kinetically prevented from further condensation.

There have been two phenomenological approaches to describing these effects. The first approach maps the (assumed random) pore network onto the random field Ising model [1,2], and these studies have had some success. However, this intuitive mapping breaks down for fluids in very regular pore structures, which show the same kinetically limited behavior as observed in amorphous pores. Another approach, which does not rely on a mapping to a known model, is the ''single pore model'' developed by Liu *et al.* [3]. In this model, macroscopic mean-field level thermodynamics are used to predict a ''plug-tube-capsule'' phase diagram for the phase-separated fluids in a single cylindrical pore. In the plug ''phase,'' the kinetics of late-time phase separation are very slow because of the large collective motions required to condense two domains into a single domain. That is, in a single pore filled with alternating plugs of two liquids it is very difficult to condense two ''like'' plugs into a larger one because the ''unlike'' liquid separating them must be removed first. In capsule phases this is not a problem, and equilibrium should be reached more quickly. The free energy driving force towards this condensation decreases very quickly with increasing plug size because the effective attraction between two plugs decreases exponentially with their separation [4]. The evaporation-condensation mechanism responsible for droplet growth in the bulk phase is nearly negligible at later times in cylindrical pores, since the surface tension of a single cylindrical plug becomes nearly independent of its size as soon as its two surfaces are far enough apart that they do not ''see'' each other. Several Monte Carlo studies of the confined Ising model using Kawasaki spin-flip dynamics have noted these effects in a qualitative way [5,6].

Relatively few molecular dynamics simulations of the phase separation of liquid mixtures in pore systems have been done. There have been several studies of two-dimensional mixtures of simple spherical particles [7–10]; these systems usually have an entirely repulsive interaction between unlike species. These studies have focused on determining growth exponents and deviations from predicted scaling behavior. However, two-dimensionally infinite systems are not comparable in these respects with one-dimensional systems like cylindrical pores, for reasons

which we explain below. Zhang and Chakrabarti [11] used molecular dynamics to study the phase separation of a two-dimensional fluid of this type in narrow channels. They found that the interfacial energy relaxed with time according to a power law with an exponent near -0.3 for times up to 1000 time units, which they attributed to purely diffusive growth. In simulations in unevenly shaped pores they found a crossover to a faster growth at later times which was attributed to hydrodynamic modes becoming important in the larger parts of the pores. We might expect that at even longer times the growth would slow again, as the asymptotic limit of the single pore model is reached. In a three-dimensional study, Zhang and Chakrabarti [12] studied a similar mixture in a cylindrical pore with dimensions $R=8.7\sigma$ and $l_z=69.6\sigma$ and observed a kinetically limited phase separation qualitatively similar to that found by Monte Carlo Ising model simulations.

Müller and Paul [13] and Albano *et al.* [14] performed extensive Monte Carlo simulations of the Ising model in a two-dimensional strip geometry using Glauber dynamics, which do not conserve the order parameter. These simulations show that phase separation in this system is entirely diffusive and can be described well by an ''annihilating random walk'' model, and that the average domain size grows in time as $t^{1/2}$ for the full length of these simulations. Unfortunately, these dynamics do not describe real liquids very well and we expect that this picture will not hold for more realistic models.

Using a Lattice-Boltzmann approach, Grunau *et al.* [15] studied the phase separation of a binary fluid in a strip geometry. These calculations support the prediction of the single pore model that phase separation slows dramatically when the domain size becomes as large as the pore size. There have also been several numerical studies of two-dimensional confined fluid mixtures using a Cahn-Hilliard approach, which predict similar behavior, and have also been used to study the effects of wetting on the phase-separation process [16–18].

From a thermodynamic standpoint, the particular case of infinite cylindrical pores is difficult to deal with in simulation studies. (In experimental systems there are no sufficiently ''infinite'' straight cylindrical micropores for this to be a problem.) It is not possible for a system that is macroscopic in only one dimension to exhibit macroscopic phase separation, because such a system is unstable with respect to formation of small domains of each phase. That is, in a confined system like a cylindrical pore (but *not* a planar pore) two phases will not separate into two very large domains separated by one interface but will form a large number of small domains. The reason is that in a long narrow pore of length L, the entropy associated with creating a ''plug'' of one domain inside the other varies as $\ln(L)$, so that $T\Delta S$ will be larger than the free energy of the two surfaces of the plug, for large enough L. In two- and three-dimensional systems, the surface tension of a domain grows with its size, so that large domains are more stable than small ones and macroscopic phase separation occurs spontaneously. In quasi-one-dimensional systems the surface tension of a large plug is nearly independent of its size and there is no driving force towards further phase separation.

In fact, simple thermodynamic models [19,20] predict that not only will the equilibrium state of such a system be a series of alternating domains, but that these domains will have some characteristic length which will vary with the temperature of the system. This length can be large enough that it does make sense to speak of phase separation in these systems, since under certain (T,X) conditions the two liquids will form long (but not macroscopic) domains which have well-defined properties per unit length. This has been demonstrated in both experimental [21–24] and simulation studies [11,25,12,26]. Rather than attempting to determine a true phase diagram by mapping out first-order transitions and a critical point, we can only determine the region of the (T,X) plane for which this ''micro-phase separation'' [24] occurs. These systems do not have true critical points, but do have a temperature where the correlation length grows to a maximum and the otherwise orderly arrangement of domains in the pore fluctuates strongly. Above this ''pseudocritical point'' the domain structure vanishes and the system becomes homogeneous along the pore axis. In computer simulation studies it is usually possible (except very near the top of the coexistence envelope) to choose the periodic cell length short enough that this micro-phase separation is suppressed, so that we can characterize the homogeneous phases directly.

At temperatures low enough that the correlation length is much smaller than the pore diameter, these systems behave like binary mixtures in three dimensions. The width of the coexistence envelope at these temperatures is fit well by the three-dimensional Ising power law prediction, and in simulation studies this can be used to estimate the ''pseudocritical'' temperature and mole fraction. For very low temperatures the Ising prediction fails for pore systems in the same way that it does for bulk systems. In the work that follows we shall refer to ''effective'' coexistence curves, phase separation, and critical points, but it should be understood that these systems do not undergo first-order transitions and do not have true critical points, and only show micro-phase separation and the remnant of critical behavior.

We have studied a symmetric Lennard-Jones binary mixture confined in a smooth cylindrical pore by a variety of computer simulation methods. We have used histogram-biasing techniques in the semigrand ensemble to determine the phase diagrams of the mixture in three different cylinders, and found that the effective critical temperature is lowered as the pore diameter is decreased. We have performed several very large quench molecular dynamics simulations in order to test the predictions of the single pore model in a realistic system. We have found that the predicted slowing down of domain growth does occur, provided that the pore is large enough and the quench temperature is deep enough. Interestingly, even in these systems we have seen a slow-growth mode at later times that is due to the slow diffusion and condensation of relatively large domains. For smaller pores and mixtures near to their effective critical points the predictions of the single pore model break down, and domains grow by a simple power law well into the asymptotic regime (where the domain length is considerably larger than the pore diameter).

This study is part of a continuing effort to understand the properties of fluid mixtures in well-characterized porous materials. Some of the quench results presented here have ap-

peared previously [25] but are shown with more recent results for easier comparison. In the current work, we have verified that these systems are only kinetically limited and that the growing domains have not reached their thermodynamic equilibrium length. We have made a series of calculations of the probability distribution of the mole fraction, $P(X)$, in different *lengths* of pore and applied a very simple thermodynamic model to these data to estimate the equilibrium domain lengths, and found that they are considerably longer than those observed in all of our quench simulations. It does not appear that any of our quench trajectories could be extended to long enough times that these equilibrium domain lengths could be observed directly, although this may be possible in a faster-equilibrating system.

In order to test the predictions of the simple thermodynamic model, we have attempted to directly measure the equilibrium domain length in our smallest pores at several temperatures by canonical Monte Carlo simulations using particle-exchange moves that greatly speed this equilibration. These calculations yield domain sizes similar to those determined from histogram data, but somewhat larger. We consider possible reasons for these differences.

II. PORE MODEL AND POTENTIAL FUNCTIONS

The fluid mixture in these simulations is a symmetric binary Lennard-Jones mixture, given by the potential function

$$U_{ij}(r)=\begin{cases} 4\epsilon_{ij}\left[\left(\frac{\sigma_{ij}}{r}\right)^{12}-\left(\frac{\sigma_{ij}}{r}\right)^{6}\right]-U_{ij}(r_c), & r\leqslant r_c \\ 0, & r>r_c \end{cases} \quad (1)$$

where $U_{ij}(r)$ is the potential between two particles of species i and j separated by a distance r. The properties of the mixture are determined by the ϵ_{ij} and σ_{ij} parameters. The mixture that we have studied is symmetric, with $\sigma_{11}=\sigma_{22}=\sigma_{12}=\sigma$, and $\epsilon_{11}=\epsilon_{22}=\epsilon$. To induce liquid-liquid phase separation we weaken the unlike-pair attractive well depth by setting $\epsilon_{12}=0.65\epsilon_{11}$. In this system particles have a slightly different ''excluded volume'' with respect to each species, which is not physical for species of identical diameter. We stress that this potential is used for reasons of simplicity and calculational convenience, and only roughly approximates a real binary mixture. The potential is ''cut and shifted'' at a distance $r_c=3\sigma$, where its value is only about 0.01ϵ. This short-range truncation of the potential greatly decreases the amount of work that must be done in each step of the calculation, since only relatively close pairs of molecules have nonzero interactions.

The pore that we use is a cylindrical hole cut out of an infinite solid of Lennard-Jones particles. By treating the solid as a continuum of fixed density, the interaction between the adsorbed molecules and the pore can be calculated as a function of radial position in the pore by using a one-dimensional lookup table [27]. (The integral over the three-dimensional solid can be solved analytically in two dimensions, but the third reduces to an elliptic function.) The potential used in this integration is not truncated, i.e., $r_c=\infty$.

The interactions between the fluid and pore are given by $\epsilon_{1W}=\epsilon_{2W}=1.277\epsilon$ and $\sigma_{1W}=\sigma_{2W}=1.094\sigma$. In addition, the density of the solid wall is $0.988\sigma^{-3}$. These parameters have previously been used to model argon adsorbed in pores of carbon dioxide [28,29]. This potential is considered ''weakly attractive'' when compared with strong adsorbates like porous carbons.

We have studied three different cylindrical pore systems and one bulk system as a reference. We have chosen the pore sizes and numbers of particles so that the ''effective'' density in each pore (and the bulk system) is the same, $\rho_{\rm eff}=0.838\sigma^{-3}$. The effective density is defined (arbitrarily) by the effective radius $R_{\rm eff}=R-\sigma/2$, which roughly accounts for the volume of the cylinder excluded by the wall-fluid potential. The three pore systems used have radii (R) of 3σ, 5σ, and 7σ; all the pore-fluid potential parameters were the same for the different pores.

In all of the results that follow, we quote quantities in Lennard-Jones reduced units [30]. For potentials of the Lennard-Jones type, the reduced temperature is expressed in ''natural'' units of ϵ/k_B. Likewise, the natural unit of length is σ, and the reduced time is measured in units of $\tau=\sqrt{\epsilon/m\sigma^2}$, with m being the mass of a particle.

III. CALCULATION OF PHASE DIAGRAMS

A. Histogram-biased semigrand ensemble method

For the case of a binary mixture in a pore, Monte Carlo simulation in the semigrand ensemble is essentially a constant $(T,\rho,\Delta\mu)$ calculation [31,32]. That is, the *number density* of particles is held fixed, but the *mole fraction* of the particles is allowed to vary. This is accomplished by including Monte Carlo moves that attempt to change a particle of one species into a particle of the other species. This ensemble is very convenient for studying liquid-liquid transitions because it does not require particle-insertion moves, which are inefficient at high density, or volume-change moves, which are expensive.

In order to determine the phase coexistence curve we use a modification of the method used by Wilding to calculate the liquid-vapor coexistence curve of the Lennard-Jones fluid [33], which is an application of the more general ''multicanonical'' approach to Monte Carlo simulation [34]. First, we perform a standard run at a temperature slightly above the expected critical point. Over this run we accumulate a two-dimensional *histogram* of the mole fraction and the energy, $H_N(X,E)$. The entries in this histogram will be proportional to the probability of observing states with that mole fraction and energy; $P_N(X,E)\propto H_N(X,E)$. The probability distribution function will depend on the system size. In the semigrand ensemble,

$$P_N(X,E)=\frac{1}{\mathcal{Y}}\exp(\beta\Delta\mu XN-\beta E)W_N(X,E), \quad (2)$$

where $\mathcal{Y}$ is the appropriate partition function and $W_N(X,E)$ is the microcanonical density of states for N particles at mole fraction X and energy E. (If $\Delta\mu=\mu_1-\mu_2$ then $X=X_1$, the mole fraction of component 1.) Factorial terms due to the indistinguishability of particles [31] are subsumed into W_N. Therefore

$$H_N(X,E)\propto\exp(\beta\Delta\mu XN-\beta E)W_N(X,E) \quad (3)$$

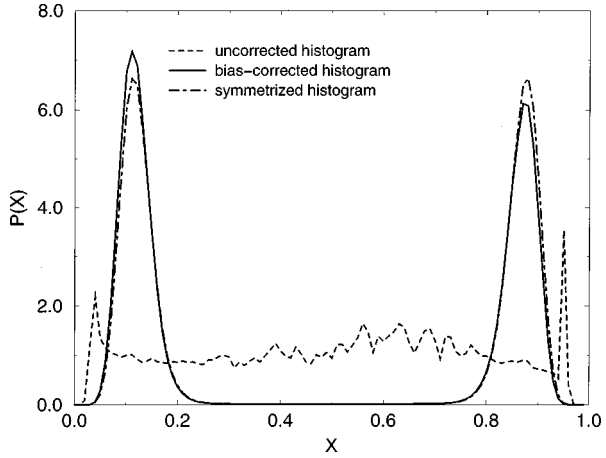

FIG. 1. Biased, unbiased, and symmetrized histograms from an $N=300$ run at $k_BT=0.95\epsilon$ in the 3σ pore system. The raw (biased) output histogram, bias-corrected histogram, and symmetrized bias-corrected histograms are shown superimposed. All three histograms have been normalized to unity.

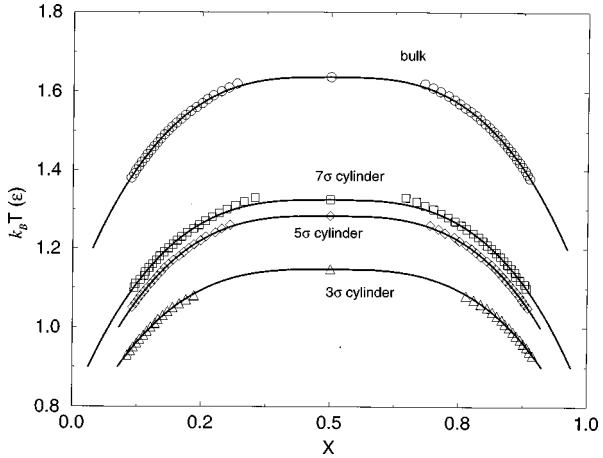

FIG. 2. (T,X) phase diagrams for all three pore systems studied. The open symbols are measured points, while the solid lines are Ising-like fits to the data.

and we can use this expression to *reweight* the measured histogram to a temperature slightly below the critical point:

$$\frac{H_N(X,E)_{\beta',\Delta\mu'}}{H_N(X,E)_{\beta,\Delta\mu}}=\exp[(\beta'\Delta\mu'-\beta\Delta\mu)XN-(\beta'-\beta)E]. \tag{4}$$

We then collapse the new histogram onto a one-dimensional histogram in X: $H'_N(X)=\Sigma_E H_N(X,E)$. We can use this new histogram as a *biasing potential* in a second Monte Carlo run at the lower temperature. Inside the coexistence region the $P_N(X)$ distribution has two peaks, which correspond to the coexisting phases. In a standard simulation the tunneling rate between these peaks is very small, so that only one peak or the other is found in a single simulation. By including this biasing potential we remove the barrier and sample *both* peaks and the region in between. In the calculation we generate states distributed according to $\exp(\beta\Delta\mu XN-\beta E)/H'_N(X)$. At the end of the simulation, having collected a new $H_N(X,E)$ histogram, we correct for the bias by multiplying the ith row of H_N, $H_N(X_i,E)$, by $H'_N(X_i)$. In exactly symmetric systems the $P(X)$ distribution should be symmetric about $X=0.5$, and we may average the two halves of the distribution to improve statistics. As an example, a set of biased, unbiased, and symmetrized histograms from a calculation in a 3σ radius pore system are shown in Fig. 1. In asymmetric systems the coexistence chemical potential difference is not trivial and we can determine the coexistence chemical potential difference by reweighting the histogram in the $\Delta\mu$ direction until the volumes under each peak are equal; this is the *equal-weight criterion* for the coexistence point [35]. This must be done at each successive temperature step. This procedure can be repeated down the coexistence line in large steps, so that five or six simulations can cover most of the liquid-liquid coexistence region [36].

B. Phase diagrams

We have calculated phase diagrams at fixed density in the (T,X) plane for all three pore systems and the bulk reference system. In order to avoid spurious effects from periodic boundary conditions along the pore axis, we have chosen the pores to be considerably longer than their effective diameters; the pore lengths were $l_z=30.375\sigma, 18.75\sigma, 13.5\sigma$, and 10.64σ, in the 3σ, 5σ, 7σ and bulk systems. The number of particles used was $N=500$, 1000, 1500, and 1000, respectively.

Histograms were taken in temperature steps of $k_B\Delta T=0.05\epsilon$ reduced units according to the procedure described above, with at least 500×10^6 Monte Carlo moves (mostly identity-exchange moves) run for each temperature. Since these systems are quick to equilibrate due to high acceptance ratios for the identity-exchange moves, we typically ran ten or 15 short independent simulations in parallel, averaging all the data after a few million moves equilibration time. These calculations were run on the IBM SP2 at the Cornell Theory Center. The resulting bias-corrected histograms were symmetrized about $X=0.5$ and used to determine $P(X)$ curves at temperature increments of $k_B\Delta T=0.01\epsilon$, from which the phase diagrams were calculated. The peak positions were determined by fitting the histogram data near each peak to Gaussian functions and locating the peaks of the Gaussians.

In order to locate the critical point, we calculated the coexistence diameter as a function of temperature and fit these data to the three-dimensional Ising-model prediction [37]. We stress that this procedure is only an approximate way of locating the *effective* critical point for the cylindrical pore systems. In bulk systems this is a fairly accurate way of determining the critical temperature [38], provided that data ''near'' to the critical temperature (in our case, usually within about 0.07 temperature units) are not used in the fit.

The phase diagrams for all four systems are shown in Fig. 2. The estimated critical temperatures for these systems are: bulk phase, $k_BT_c\simeq1.64\epsilon$; 3σ cylinder, $k_BT_c\simeq1.15\epsilon$; 5σ cylinder, $k_BT_c\simeq1.28\epsilon$; and 7σ cylinder, $k_BT_c\simeq1.33\epsilon$. As the cylinder size is decreased, the critical temperature is reduced considerably. Note that these different systems are comparable only in density; at a given temperature, their internal energies are quite different (due to the different radii of the pore-fluid potentials) so that the confined fluids are not in equilibrium with each other.

IV. QUENCH MOLECULAR DYNAMICS

We have performed five different quench experiments in this study. Some analysis of two of these runs was published previously [25]. Three of these runs were done to determine the effects of quench temperature on the domain growth process; these three were run at $k_BT=0.75\epsilon$, 1.00ϵ, and 1.10ϵ in the 3σ pore. We have also run trajectories in 5σ and 7σ pores at $k_BT=1.00\epsilon$, to determine the effect of increasing pore size at fixed temperature.

A. Details of molecular dynamics calculations

In each quench study the system was equilibrated at a high temperature ($k_BT=5.0\epsilon$) for at least 30 000 time steps using a Gaussian isokinetic thermostat. The system was then quenched to a temperature in the two-phase region in a single step by changing the thermostat temperature, and the integration was continued for between 600 000 and 2.25×10^6 more time steps, still using the Gaussian thermostat. The length of a single time step was 0.005τ, and we used a third-order Gear finite difference algorithm for the integration. (Equilibrium calculations were also done with fifth-order Gear algorithms, and we could detect no difference in the fluid properties between these two algorithms.)

The data shown for the single 5σ system are an average over nine independent runs of smaller systems of length 187.5σ ($N=10\,000$). The data shown for the $k_BT=1.00\epsilon$, 3σ system are an average over eight independent runs of smaller systems of length 562.5σ ($N=9258$). The other three systems were run as single trajectories, each with $N=100\,000$. l_z in the 3σ, 5σ, and 7σ pores was 6075.8σ, 1875σ, and 900σ, respectively.

All the quench calculations were done with a parallel molecular dynamics code based on a one-dimensional domain decomposition algorithm. For the smaller systems studied ($N\simeq10\,000$) we used 15 or 20 processors, and for the larger ($N=100\,000$) systems we used 64 processors. In the larger systems, we could typically get between 250 000 and 300 000 steps into a single 20 hour run, depending on the pore diameter. These calculations were all run on either the IBM SP2 at the Cornell Theory Center or the Cray T3D at the Pittsburgh Supercomputer Center. The total CPU time used by the quench calculations was approximately 18 000 hours.

We have used two different measures to monitor the phase-separation process. The first is $E(t)-E_0$, the total potential energy per particle of the system relative to a fully relaxed state, the homogeneous phase at saturated concentration. After an initial decay of transients this quantity effectively measures the interfacial area in the system, which is inversely proportional to the domain size for these systems. The reference state energy for each pore system was determined in a separate simulation, using a canonical Monte Carlo run in a short cylinder at a mole fraction determined from the phase diagrams measured earlier.

The second measure is the average domain size. We can define a local selectivity (dependent on time and the z coordinate) by

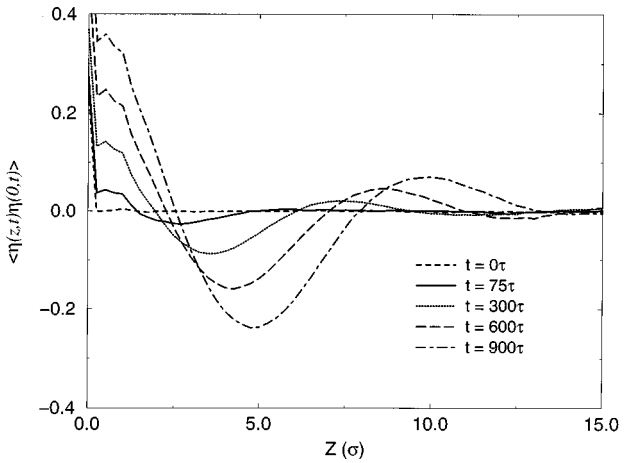

FIG. 3. Autocorrelation of local selectivity, for several times in the $k_BT=0.75\epsilon$ quench run in the 3σ radius cylinder system. At later times, the position of the first minimum moves to larger z, and the amplitude of the oscillation increases. The z discretization is 0.25σ; the small oscillations at $z\leqslant2.5\sigma$ are due to correlation in the liquid structure.

$$\eta(z,t)=\frac{\rho_1(z,t)-\rho_2(z,t)}{\rho_1^0+\rho_2^0}, \tag{5}$$

where $\rho_1(z,t)$ is a short-time averaged density of component 1 at position z, ρ_1^0 is the system-averaged density of component 1, etc. We then calculate the autocorrelation function of η in the z direction, $\langle\eta(z,t)\,\eta(0,t)\rangle$. The position of the first minimum of this function, referred to as $l(t)$, is characteristic of the domain size and is the one-dimensional analog of the scaling form used in two and three dimensions [7]. As an example, a set of autocorrelation functions from the quench to $k_BT=0.75\epsilon$ in the 3σ radius pore system are shown in Fig. 3. Large-scale simulations are necessary because the quality of data is determined by the number of domains, which is much smaller than the number of particles. We have attempted to use cluster-counting routines [30] to determine the distribution of domain sizes, but found that because of the relatively diffuse interfaces these definitions were extremely sensitive to cutoff parameters and were not reliable.

In order to visualize the domain growth process, we also plot a coarse-grained one-dimensional mole fraction as a function of z and time. That is, we average the mole fraction in a 1σ section of pore over a few hundred time steps; if the total average is greater than 0.5, we plot a point, if it is less than 0.5, we leave a space. These ''snapshots'' are then laid side by side, as shown in Fig. 8. This format is a convenient way to visualize a large number of large molecular configurations side by side.

B. Variation of quench behavior with temperature

The domain sizes as functions of time for the three quench experiments in the 3σ radius pore are shown in Fig. 4. At short times, all three curves follow a power law growth, with larger exponents for higher quench temperatures. The short-time growth exponent in the $k_BT=0.75\epsilon$ quench is 0.212 ± 0.006, in the $k_BT=1.00\epsilon$ quench it is 0.212 ± 0.003, and in the $k_BT=1.10\epsilon$ quench it is

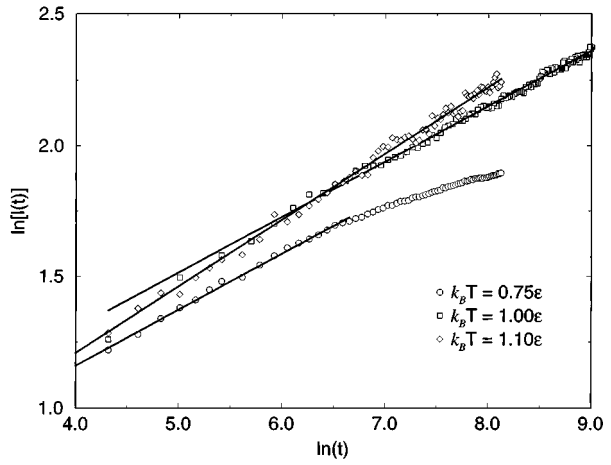

FIG. 4. Growth in average domain size $l(t)$ with time after quench, for the 3σ cylinder at $k_BT=0.75\epsilon$, 1.00ϵ, and 1.10ϵ.

0.254 ± 0.007. As the temperature is increased, the $l(t)$ data becomes noisier. This is caused by increasingly diffuse domain boundaries and larger fluctuations in the liquid. At later times, the $k_BT=1.00\epsilon$ and 1.10ϵ quenches continue to follow their early-time power law growth, while the deepest quench crosses over to what appears to be a second power law with exponent 0.119 ± 0.004. (Over this range of time these data are fit well by a power law form; at later times the growth may slow further.)

The corresponding energy relaxation data for all three quenches in the 3σ pore are shown in Fig. 5. These data show the same qualitative trends as the $l(t)$ data for these systems. The short-time relaxation exponents are -0.255 ± 0.001, -0.216 ± 0.005, and -0.327 ± 0.002 for the $k_BT=0.75\epsilon$, 1.00ϵ, and 1.10ϵ quenches, respectively. The energy relaxation exponents for the $k_BT=0.75\epsilon$, and 1.10ϵ quenches are slightly larger than expected. The late-time exponent for the $k_BT=0.75\epsilon$ system is -0.122 ± 0.004, in good agreement with the $l(t)$ data.

In all of these quench experiments, the relaxation exponents measured from the energy data depend strongly on the choice of reference energy E_0. Because the two fluid components are reasonably soluble in each other, accurately determining E_0 requires knowing the saturation concentrations, so that small errors in our phase diagram calculations may be magnified into large errors in our energy relaxation exponents. Although the data may be fit well by the power law, the uncertainty in the exponent calculated from a χ^2 fitting procedure does not reflect this possible systematic error due to the use of a reference energy.

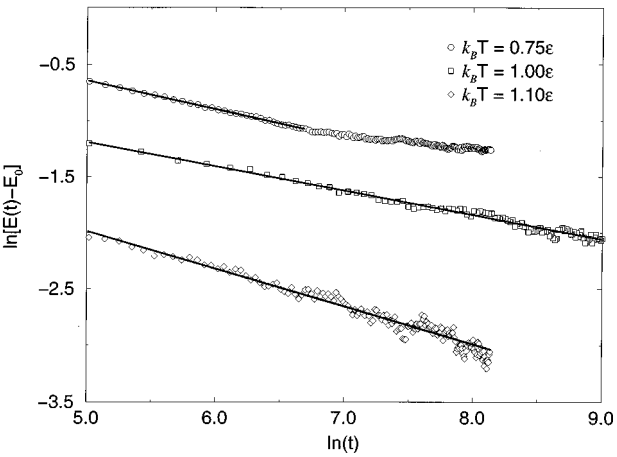

FIG. 5. Energy relaxation vs time after quench, for the 3σ cylinder at $k_BT=0.75\epsilon$, 1.00ϵ, and 1.10ϵ.

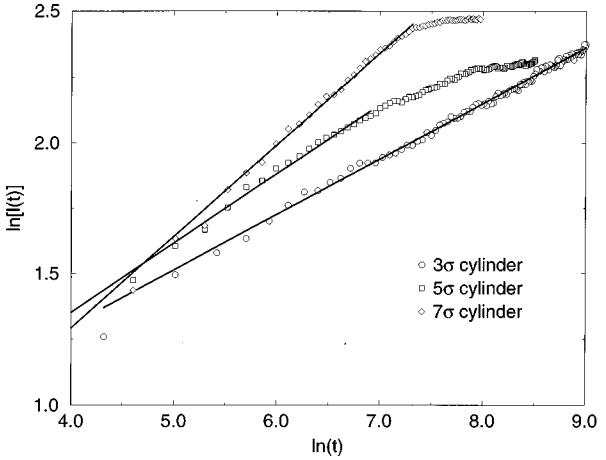

FIG. 6. Average domain size $l(t)$ vs time after quench, for all three cylinders at $k_BT=1.00\epsilon$.

From the quench data at different temperatures, we conclude that the growth exponents in these systems are weakly dependent on temperature, and that the presence of a crossover to a slow mode at late times only occurs if the temperature is far enough below the critical point that the interfaces between domains are well defined on a small length scale.

C. Variation of quench behavior with pore size

The average domain sizes as functions of time after the quench for all three systems at $k_BT=1.00\epsilon$ are shown in Fig. 6. In all three pores the domains grow according to a power law at short times. The exponent for this growth in the 7σ cylinder is 0.35 ± 0.01, the exponent in the 5σ cylinder is 0.27 ± 0.01, and the exponent in the 3σ pore is 0.212 ± 0.003. For larger pores, the short-time exponent is larger. This can be compared with previous simulations of bulk phase-separation behavior, in which the domain size in critical quenches was found to grow with a much larger exponent. Ma *et al.* measured a value of 0.6 ± 0.1 for this exponent [39], while more recent (and larger) simulations of a slightly different system by Laradji *et al.* found an exponent of 1.0 [40]; the discrepancy may be due to the two simulations reaching different asymptotic behaviors at different times [40].

At later times, in the two larger pores there is a distinctive slowing in the growth rate. In the larger 7σ system this crossover is quite sharp and occurs at $l(t)\simeq11\sigma$, while in the smaller 5σ pore it happens more gradually, beginning when $l(t)\simeq9\sigma$. In the smallest cylinder the original power law behavior persists unchanged to the longest times we were able to simulate.

The corresponding energy relaxation data for the three systems at $k_BT=1.00\epsilon$ are shown in Fig. 7. The same general trends occur in these data as in the $l(t)$ data; for larger pores, the crossover to slow relaxation at later times is

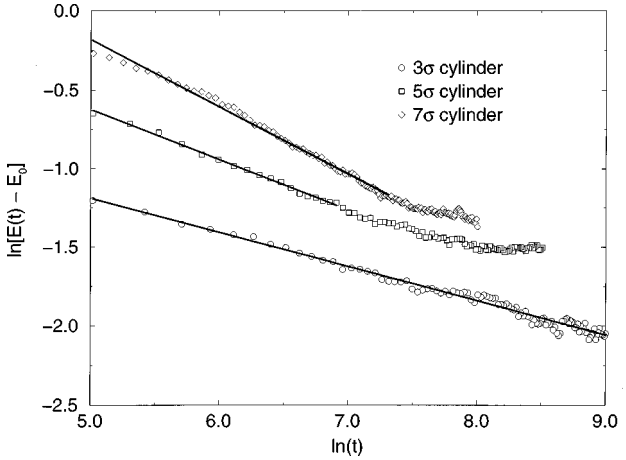

FIG. 7. Energy relaxation vs time after quench, for all three cylinders at $k_BT=1.00\epsilon$. In order that the data not overlap, the 7σ pore data have been shifted *up* by 0.5 and the 5σ pore data have been shifted *up* by 0.25.

sharper and the initial relaxation exponent is larger. The exponents for the energy relaxation in the three systems are -0.216 ± 0.005, -0.32 ± 0.01, and -0.426 ± 0.002 in the 3σ, 5σ, and 7σ systems, respectively. As the pore diameter is increased, the agreement between the domain size and energy relaxation exponents becomes poorer. This fast relaxation of the energy may be caused by the gradual crossover from three-dimensional to one-dimensional growth. As domains grow to block the width of the pore, their liquid-liquid interfaces are quickly replaced by liquid-solid (pore) interfaces, as their shape changes from irregular to cylindrical. So, as large, irregularly shaped domains become cylindrical plugs their contact area with the other phase is greatly reduced, even though their average length may not change much. In fact, the ratio of (absolute) exponents in the 5σ pore is only about 1.18 to 1, while in the 7σ pore the ratio is 1.22 to 1, so that this is not an extreme effect. The 3σ pore appears to be within the one-dimensional regime, and the exponents agree.

D. Domain growth mechanism

In Fig. 8 we plot coarse-grained domain profiles of the three quench trajectories at $k_BT=1.00\epsilon$, in order to determine the mechanism of domain growth at later times. At short times, each system consists of a large number of small domains which quickly condense into slightly larger domains. At later times it is clear that in the 5σ and 7σ pore systems all further growth occurs via a relatively small number of condensation events, where two neighboring domains merge into one larger domain. In the smallest cylinder, this process is not as obvious. Since domain growth in this system occurs with a smaller power law exponent but over a longer length scale, we believe that there must be a relatively slow transfer of mass from smaller domains to larger domains by diffusion.

E. Short-time relaxation of energy

We have noted that for very short times the energy relaxation in all five quench systems does not follow a power law but a more complex form. [Since we only measure the $l(t)$ data every 50 or so time units, we do not observe this there.] The short-time energy relaxation data for all five trajectories are shown in Fig. 9. All the curves have a very similar shape, and all of the systems begin to follow simple power law relaxation at about the same time after quenching, $t\simeq150\tau$ [$\ln(t)\simeq5$]. This relatively slow relaxation at short times may be due to the aftereffects of the very fast quench at $t=0$, so

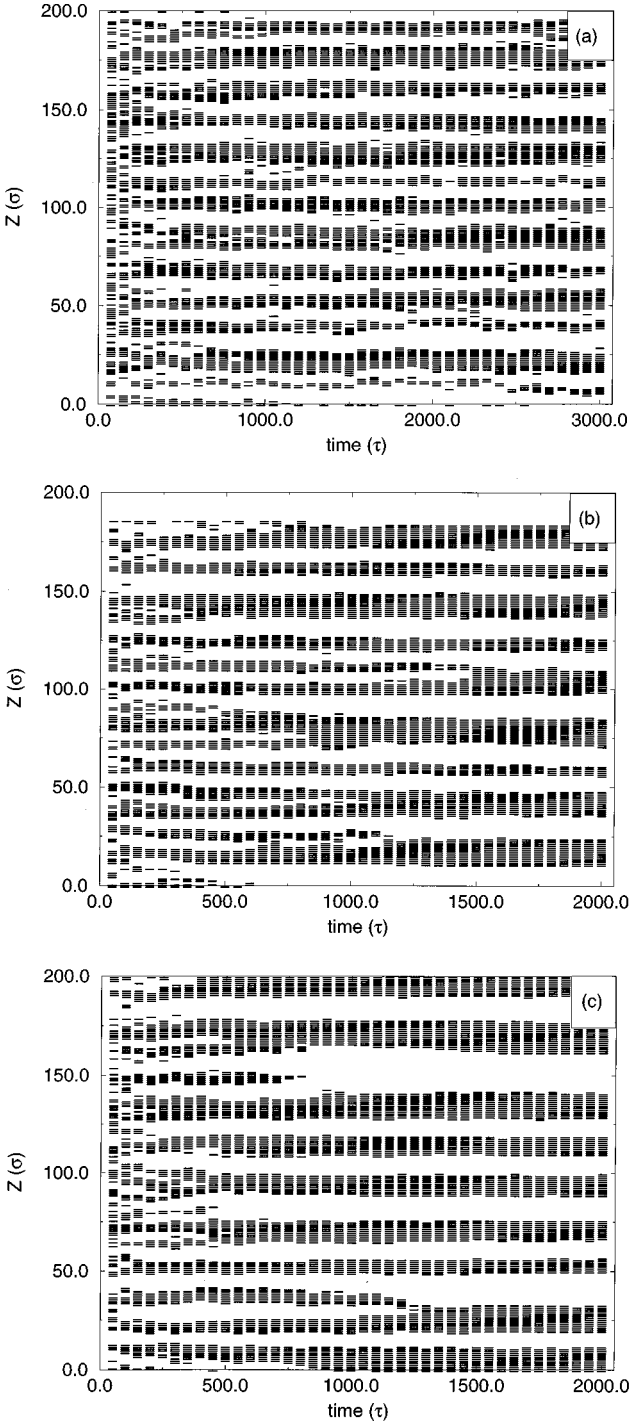

FIG. 8. Coarse-grained domain profiles from the quench simulation in the (a) 3σ, (b) 5σ, and (c) 7σ pore systems at $k_BT=1.00\epsilon$. The black bars are domains rich in one component, white spaces domains rich in the other. The x axis is the simulation length; each pore ''snapshot'' is an average over 500 steps, at a spacing of 15 000 steps between snapshots.

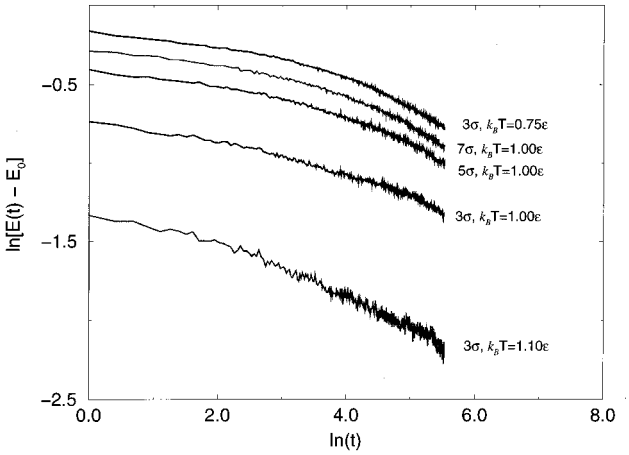

FIG. 9. Short-time energy relaxation data for all five quench runs. The energy relaxation for the first 50 time units is quite slow, followed by a gradual crossover to linear behavior at around $t=150\tau$ [$\ln(t)\simeq 5$].

that the ''local'' liquid structure in these systems takes about this long to equilibrate at the quench temperatures. For this reason, in all of our curve fitting to the energy relaxation data, we have only used the data taken *after* $t=150\tau$.

V. ANALYSIS OF $P(X)$ HISTOGRAMS

A. Simple theory of one-dimensional behavior

The thermodynamics of one-dimensional systems of molecules having finite-ranged interactions prohibit macroscopic phase transitions. The classic argument for this [19] is that we can write the free energy of a two-phase, one-dimensional system (ignoring effects from interactions between interfaces) as

$$F-F_0=nT\ln\left(\frac{n}{eL}\right)+n\gamma, \tag{6}$$

where L is the length of the system, n is the number of interfaces (and in a periodic system, the number of domains), and γ is the surface tension. The logarithmic term is the entropy due to the motion of the domains. F_0 is the free energy of the fully relaxed (e.g., phase-separated) system. For large L, the entropy associated with domain motion will always be larger than the total surface tension, so that macroscopic phase separation will not occur and the system will consist of microscopic domains of some equilibrium length L/n.

In order to estimate the average size of these domains, we introduce a scale factor to fix the units of L; by setting $BL'=L$ we get

$$F-F_0=nT\ln\left(\frac{n}{L'}\right)+nT\ln\left(\frac{1}{Be}\right)+n\gamma \tag{7}$$

$$=n\left[T\ln\left(\frac{n}{L'}\right)+C\right], \tag{8}$$

where the surface tension and scale factor have been absorbed into C. So, if we can determine $F-F_0$ and C, we can determine the equilibrium domain length. By differentiating the above expression with respect to n we end up with

$$\frac{\partial(F-F_0)}{\partial n}=C+T+T\ln\left(\frac{n}{L'}\right), \tag{9}$$

which we set equal to zero, and get

$$\ln\left(\frac{L'}{n}\right)=\frac{T+C}{T}. \tag{10}$$

B. Calculation of equilibrium domain sizes from histogram data

We expect that the equilibrium domain length in a phase-separated system, although microscopic, will be large on a molecular scale. Therefore in a small system at equilibrium there would never be more than two domain walls (so that the system is fully phase separated). We can apply this simple model to such a system and use it to calculate the value of C, which should be independent of system size for systems long enough that the interfaces do not strongly interact.

From the histogram-biased Monte Carlo simulations described above we have determined $P(X)$ in many such systems. These histograms all have similar shapes. There are two peaks, one corresponding to each phase, and a broad, very flat region between the two peaks, which corresponds to phase-separated states with total mole fractions between those of the two homogeneous phases. The *area* of this region is proportional to the free energy of the phase-separated system. Since the areas of the single peaks (which are equal) are proportional to the free energies of the homogeneous phases, the ratio of these areas gives us the free energy difference $F-F_0$. More specifically, if P is the area of the interfacial region and P_0 is the area of one of the peaks, then $F-F_0=-T\ln(P/P_0)$.

In practice, we estimate the area of the interfacial region by multiplying the height of the normalized histogram at midpoint by the distance between the two equilibrium peaks; $P\equiv H_{\mathrm{mid}}(X_2-X_1)$. That is, the interfacial contribution to the full $P(X)$ distribution is assumed to be rectangular. Since we are only considering symmetric systems and the $P(X)$ distribution is normalized, the area of one peak is then just $(1-P)/2$ and the calculation of C is simple, since we know the pore length L' in reduced units and there are two interfaces.

C. Results

In the 3σ cylinder we have obtained $P(X)$ histograms for $k_BT=0.95\epsilon$, 0.975ϵ, 1.00ϵ, 1.025ϵ, and 1.05ϵ, in pores with $N=100$, 300, 500, 700, and 900 ($l_z=6.075\sigma$ through $l_z=54.675\sigma$). All of these histogram runs were of lengths similar to those used for the phase diagram calculations. In Fig. 10 are some of the $P(X)$ distributions from these runs. The histogram peaks show the expected behavior; as the system is made larger at a single temperature the peaks become sharper and shift to slightly higher mole fraction [41,42],

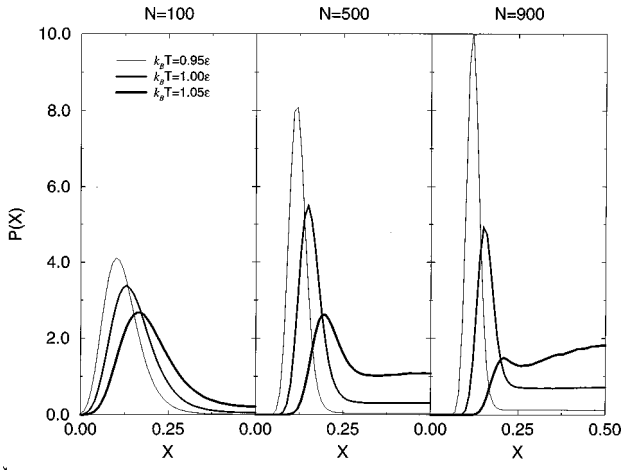

FIG. 10. Bias-corrected histograms from the thermodynamic study of domain sizes in the 3σ pore system at several temperatures. Three different *lengths* of pore are shown, containing 100, 500, and 900 fluid particles.

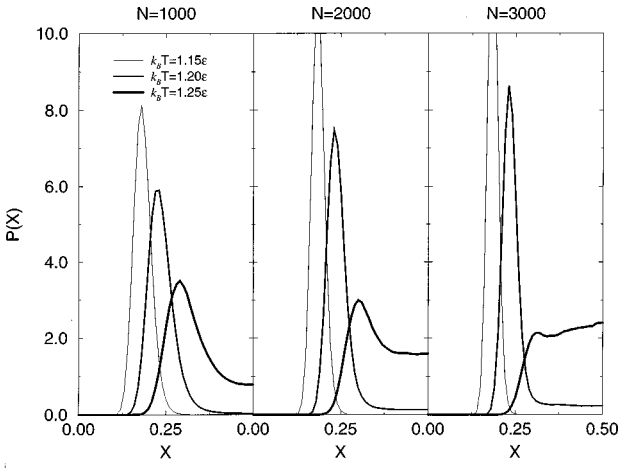

FIG. 11. Bias-corrected histograms from the thermodynamic study of domain sizes in the 5σ pore system at several temperatures. Three different *lengths* of pore are shown, containing 1000, 2000, and 3000 fluid particles.

while as the temperature is raised in a single pore the peaks become broader and the peak location moves towards $X=0.5$, its critical value.

In the two larger systems, the region of the curve between the two peaks is visibly flat, as predicted by our simple model. As the temperature is raised, the $P(X)$ value at the midpoint of this flat region increases, indicating that the probability of observing the system in a two-phase state is increasing relative to the probability of observing it in a one-phase state. As the temperature is brought near to the critical temperature, especially in the largest pore, the flat region around $X=0.5$ begins to bulge upwards. This is caused by there being *more than two* domains in the system; near the critical temperature the domain length can be fairly small, and for X near to 0.5 there might be, say, four domains in the periodic system. For X further away from 0.5, these ''extra'' domains would have to be very small. Due to the nonzero width of the domain interfaces in the real system this is unfavorable, so that ''extra'' domains only contribute to the entropy near $X=0.5$, and we see a broad peak in $P(X)$. At lower temperatures this does not occur because the domain lengths will be much larger and these relatively short pores will only hold two domains.

In the 5σ cylinder we have measured $P(X)$ histograms for $k_BT=1.10\epsilon$, 1.15ϵ, 1.20ϵ, and 1.25ϵ for systems with $N=400$, 1000, 2000, and 3000 particles, with system lengths between $l_z=7.5\sigma$ and $l_z=56.25\sigma$. These histograms have all the same qualities as those in the smaller cylinder. A selection of these data is shown in Fig. 11, and follows all of the same trends as the 3σ histograms, even showing a small bulge in the $P(X)$ data near $X=0.5$ for the largest system at the highest temperature.

In both cylinders we have measured the equilibrium domain length as a function of temperature using the scheme described above. In each case we calculated C at each temperature in all of the different pore sizes studied, in order to determine if there were higher-order effects that our simple theory was missing (which would result in C being dependent on system size). In all cases, for pores of length greater than 10σ the values of C showed only a weak dependence on domain size, if any. For instance, in the 3σ pore at $k_BT=0.95\epsilon$, the values of C calculated in the $N=300$, 500, 700, and 900 systems were 3.82, 3.88, 3.86, and 3.89, respectively. For each temperature in the 3σ pore, we have used the average value of C over these systems to determine the equilibrium pore length. (In the 5σ pore, we have averaged over the $N=1000$, 2000, and 3000 C values.)

The estimated equilibrium domain lengths from these calculations are shown in Fig. 12, along with equilibrium domain lengths determined from direct Monte Carlo simulations (described in the next section). A logarithmic scale is used to show all the data on one graph. In the smaller pore the estimated domain sizes range from $l_{\rm eq}=158\sigma$ at $k_BT=0.95\epsilon$ to $l_{\rm eq}=24.7\sigma$ at $k_BT=1.05\epsilon$. In the larger pore the equilibrium domain lengths are much larger at these temperatures but become quite small near to the critical temperature, ranging from $7\times10^5\sigma$ at $k_BT=1.05\epsilon$ down to 24.9σ at $k_BT=1.25\epsilon$, only slightly below the critical temperature. These lengths show that none of our quench molecular dynamics runs were near to their equilibrium states at the end

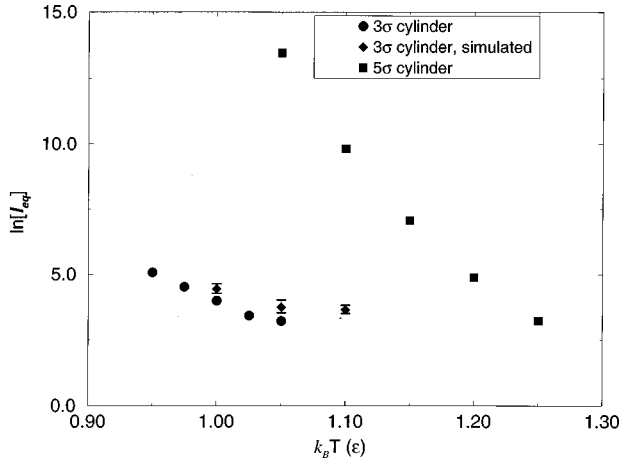

FIG. 12. Results from histogram analysis for the equilibrium domain length in the 3σ and 5σ pore systems, and from direct Monte Carlo simulation of the equilibrium domain length in the 3σ system, over a range of temperature.

of the trajectories. It might be possible for a longer run in the 3σ system at $k_BT=1.10\epsilon$ to come to thermodynamic equilibrium, but this would probably require a trajectory of more than 10×10^6 steps, which is currently not feasible for a system of 10^5 particles.

VI. EQUILIBRIUM MONTE CARLO SIMULATIONS

We have already explained that equilibrium domain sizes cannot be estimated directly from molecular dynamics simulations because these simulations are kinetically limited and cannot reach true thermodynamic equilibrium in reasonable simulation times. Also, the equilibrium lengths predicted from the histogram data are quite large, even for temperatures near to the critical point. By using a simulation technique that equilibrates faster such a direct determination may be possible, at least for some of these systems.

We have performed canonical Monte Carlo simulations in a 3σ pore system at several different temperatures in order to verify this. These simulations consisted of two different kinds of moves: the usual Monte Carlo displacement moves, and moves where two particles of different species are exchanged. [It is simple to show that the acceptance criteria for these exchange moves is just $\exp(-\beta\Delta E)$ as usual, provided that both particles are chosen randomly.]

Each simulation was run for 200 000 Monte Carlo cycles, with each cycle consisting of 8000 particle-displacement moves and 2000 particle-exchange moves. The system consisted of 9258 particles at $X=0.5$ in a 562.5σ long, 3σ radius pore, as used in one of the quench molecular dynamics runs. Because the Monte Carlo method is not easily parallelized these calculations were run on workstations; each took approximately 350 hours to complete. At the end of each simulation the data were analyzed to calculate domain lengths in the same way that $l(t)$ data were measured from the quench trajectories.

We have run three different temperatures in this way. The lowest temperature, $k_BT=1.00\epsilon$, gave an equilibrium domain length estimate of $l_{\mathrm{eq}}=84\sigma\pm15\sigma$. Coarse-grained domain profiles from this calculation are shown in Fig. 13(a). Because the domains are so large there are very few in the system at any one time, and our average value may be a poor estimate. Furthermore, we see from the profile data that the correlation time in this system is quite long, so that successive blocks of 5000 Monte Carlo cycles are highly correlated, which also reduces the quality of this average.

In Fig. 13(b) are the coarse-grained domain profiles from a Monte Carlo run at $k_BT=1.05\epsilon$. The average domain length from these data is $l_{\mathrm{eq}}=42\sigma\pm10\sigma$. This system also shows considerable correlation between successive block averages, especially at earlier ''times.'' The last Monte Carlo run was done at $k_BT=1.10\epsilon$, which gave an equilibrium domain size of $l_{\mathrm{eq}}=38\sigma\pm6\sigma$. Domain profile data from this calculation are shown in Fig. 13(c).

These estimated values are shown alongside those calculated from histogram data in Fig. 12. The directly measured values appear to be less temperature dependent than the data calculated from the histograms and are systematically slightly larger. One possible source for this discrepancy is the approximations that we have made in applying the simple thermodynamic model described above. The first approximation is that the interfaces in the system have zero width and do not interact. This is nearly true for very long systems at low temperatures, but as the temperature is raised the surface tension is lowered and the domain boundaries become much broader. The effect of this broadening is to *reduce* the entropy of the real system, so that the model will overestimate

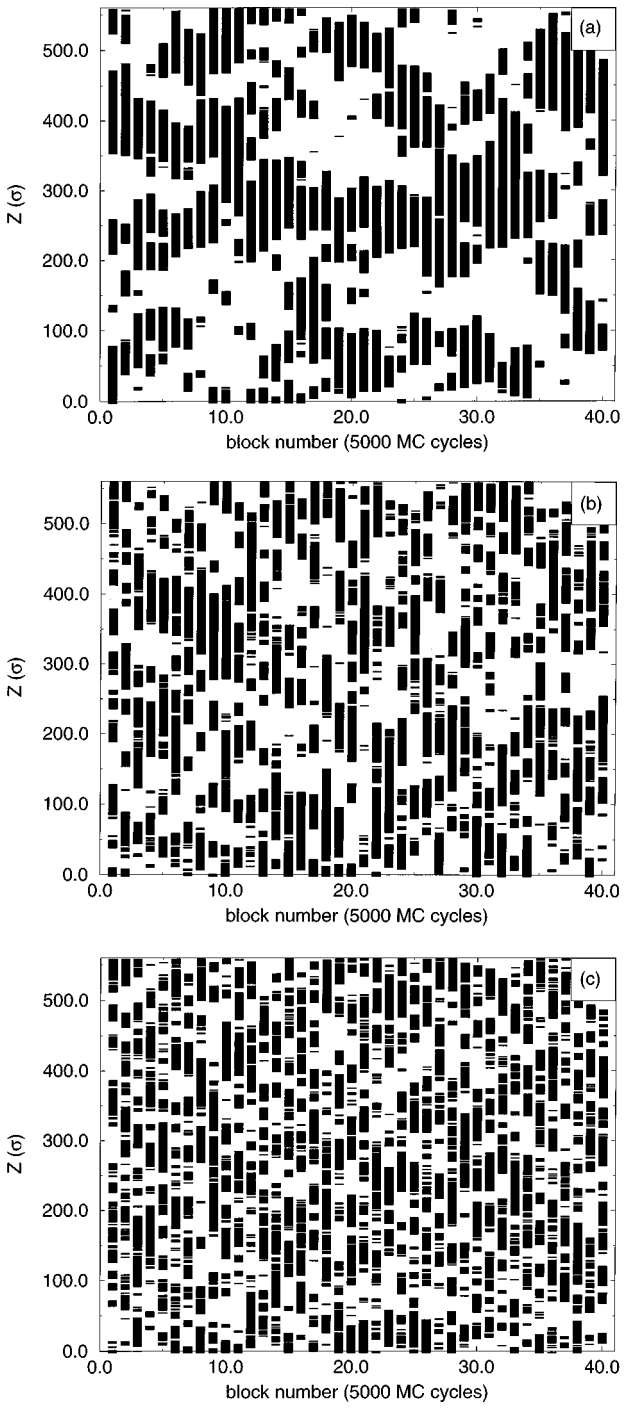

FIG. 13. Coarse-grained domain profiles from Monte Carlo simulations in the 3σ pore system at (a) $k_BT=1.00\epsilon$, (b) $k_BT=1.05\epsilon$, and (c) $k_BT=1.10\epsilon$. The black bars are domains rich in one component, white spaces domains rich in the other. The x axis is the simulation length; each pore ''snapshot'' is an average over 5000 Monte Carlo cycles.

this value and underestimate the average domain length. This is a temperature dependent correction and will be more important at higher temperatures, which may account for the discrepancy in the temperature dependence of the two sets of data. Because we have no simple way to estimate the interfacial widths in the system, applying this correction in a meaningful way is difficult.

The other major approximation made in applying the simple model to these systems was the assertion that $P \equiv H_{\mathrm{mid}}(X_2 - X_1)$. This is an arbitrary decomposition of the histogram into interfacial and homogeneous parts and almost surely *overestimates* P, since we have not taken into account the width of the homogeneous phase peaks. Therefore this approximation *also* overestimates the entropy in the system and underestimates the equilibrium domain size. This error should be less dependent on temperature than the one described above. Correcting for this would be somewhat arbitrary without a detailed theory of the shape of the histograms.

VII. DISCUSSION

Although computer simulations of confined systems benefit from a relative lack of finite-size effects due to periodic boundary conditions and small system sizes, cylindrical pore systems pose special problems, especially at temperatures near the top of the phase envelope. With some caution, the usual concepts of phase transitions can be applied here but these interpretations break down when the one-dimensional nature of the system begins to strongly influence its behavior. Nevertheless, useful information about the thermodynamics of liquid mixtures in cylindrical micropores can be obtained in this way.

In reasonably large micropores (more than a few tens of molecular diameters thick) many of these problems are academic; the temperature range over which these one-dimensional effects are visible is extremely small and is not observable using present molecular simulation techniques. In these pores finite-size scaling theories can be applied to estimate the shift in critical temperature and pressure [42]. These theories are very successful at describing critical point shifts due to confinement, but are applicable only when the scale of confinement is large relative to the scale of atomic interactions, so that the shifts are small. In the small pores that we have studied this condition fails; the liquid is highly structured even in the center of the pore and the shifts in critical parameters from their bulk values are large.

We have demonstrated that by using a very simple thermodynamic model reasonable estimates of the equilibrium domain sizes in these systems can be obtained from $P(X)$ data from Monte Carlo simulations. Although obtaining the $P(X)$ data requires long simulations in fairly large systems, the analysis of these data is simple and gives good results. We have shown that this model is consistent over a range of pore sizes, lengths, and temperatures, in that the predicted equilibrium domain lengths are not systematically dependent on the pore lengths used in the simulation (except in the shortest pores used) and that the histograms we have measured have the expected shapes for all systems except large ones close to the critical temperature. Introducing greater realism into the model by including nonzero interfacial widths is not difficult, except in calculating the appropriate widths. We have tried this for a few of the systems studied and found that the effects of introducing interfaces 5σ and 10σ wide are relatively small, so that the predicted equilibrium domain lengths only change by 10% or 20%.

We have also shown that directly determining the equilibrium domain sizes is possible via Monte Carlo simulations, at least in small pores relatively near to their critical points. It is likely that extremely long simulations in larger systems will be required for accurate results. The data we have so far show somewhat longer domains than the thermodynamic model does, which appears to be due to a systematic overestimation of the entropy in the thermodynamic model. The Monte Carlo approach to calculating domain sizes would also allow calculation of the equilibrium *domain size distribution*, which is not immediately accessible from the $P(X)$ data.

The main conclusion that we draw from the quench molecular dynamics part of this study is that the picture of phase-separation kinetics obtained from the single pore model (and supported by a number of simulations of liquids and Ising models in large pores) appears to break down for sufficiently narrow pores. We have studied several different pore sizes and temperatures to better characterize this behavior.

In very small pores, for temperatures near enough to the apparent critical point there is no crossover to a slow-growth mode. This is due to the increased mobility and width of the domain interfaces at higher temperatures. We have only observed this directly in the smallest (3σ) pore studied, but expect that it would also be true in the 5σ pore for a quench temperature much closer to the pore critical point.

As we make the pores bigger, the behavior at short times approaches that of a bulk system. This is indicated by an increase in the growth exponents. In the largest pore we studied the growth exponents are far from their predicted bulk values, indicating large confinement effects even in 7σ radius pores.

At short times there is a slow relaxation of the energy that appears to be relatively independent of the pore size or temperature. We believe that this is due to the local relaxation of the liquid structure, especially near the pore walls where the liquid is highly ordered. Since all the systems we have simulated cross over to the power law growth at nearly the same time, this relaxation seems to be unaffected by temperature or pore size. Since this relaxation is *slower* than the energy relaxation due to phase separation, we note that the phase-separation process apparently does not begin until the liquid is mostly relaxed at the lower temperature.

Lastly, the coarse-grained domain profiles from the quench studies suggest that the principal domain growth mechanism at all but the earliest times is the condensation of neighboring domains. This process is not very visible in the smallest pore, which is the only pore for which the kinetic slowing at late times is *not* observed, which suggests that in the smaller pores (or pores close to their critical temperatures) there is a second growth mechanism.

In summary, we have studied a binary fluid mixture adsorbed in simple cylindrical pores by quench molecular dynamics, histogram-biased semigrand Monte Carlo, and canonical Monte Carlo simulations. We have characterized the

effects of both quench temperature and pore size on the kinetics of phase separation in these systems, and found that while our results support some of the predictions of earlier work in larger pores, for sufficiently small pores these predictions break down. We have also applied a simple thermodynamic model to calculate the equilibrium domain sizes in these systems from histogram simulation results, and found reasonable agreement with direct simulations.

ACKNOWLEDGMENTS

We thank the Petroleum Research Fund of the American Chemical Society for their support of this work, the National Science Foundation for a Metacenter grant (Grant No. MCA93S011P) which made these calculations possible, and the Cornell Theory Center and Pittsburgh Supercomputer Center for their general assistance. L.D.G. would like to thank the National Science Foundation for financial support.

[1] D. S. Fisher, Phys. Rev. Lett. **56**, 416 (1986).
[2] J. Villain, J. Phys. (France) **46**, 1843 (1985).
[3] A. J. Liu, D. J. Durian, E. Herbolzheimer, and S. A. Safran, Phys. Rev. Lett. **65**, 1897 (1990).
[4] T. Nagai and K. Kawasaki, Physica A **120**, 587 (1983).
[5] A. J. Liu and G. S. Grest, Phys. Rev. A **44**, R7894 (1991).
[6] L. Monette, A. J. Liu, and G. S. Grest, Phys. Rev. A **46**, 7664 (1992).
[7] E. Velasco and S. Toxvaerd, Phys. Rev. Lett. **71**, 388 (1993).
[8] P. Ossadnik, M. F. Gyure, H. E. Stanley, and S. C. Glotzer, Phys. Rev. Lett. **72**, 2498 (1994).
[9] E. Velasco and S. Toxvaerd, Phys. Rev. E **54**, 605 (1996).
[10] P. Keblinski, W.-J. Ma, A. Maritan, J. Koplik, and J. R. Banavar, Phys. Rev. E **47**, R2265 (1993).
[11] Z. Zhang and A. Chakrabarti, Phys. Rev. E **52**, 2736 (1995).
[12] Z. Zhang and A. Chakrabarti, Phys. Rev. E **50**, R4290 (1994).
[13] M. Müller and W. Paul, J. Stat. Phys. **73**, 209 (1993).
[14] E. V. Albano, K. Binder, D. W. Heerman, and W. Paul, Physica A **183**, 130 (1992).
[15] D. W. Grunau, T. Lookman, S. Y. Chen, and A. S. Lapedes, Phys. Rev. Lett. **71**, 4198 (1993).
[16] A. Bhattacharya, M. Rao, and A. Chakrabarti, Phys. Rev. E **49**, 524 (1994).
[17] A. Chakrabarti, Phys. Rev. Lett. **69**, 1548 (1992).
[18] S. Puri and K. Binder, J. Stat. Phys. **77**, 145 (1994).
[19] L. D. Landau and E. M. Lifshitz, *Statistical Physics*, 3rd ed. (Pergamon Press, Oxford, 1959), Vol. 1, translated by J. B. Sykes and M. J. Kearsley.
[20] T. L. Hill, *Statistical Mechanics, Principles and Selected Applications* (McGraw-Hill Book Co., Inc., New York, 1956).
[21] M. Y. Lin, S. K. Sinha, J. M. Drake, X.-I. Wu, P. Thiyagarajan, and H. B. Stanley, Phys. Rev. Lett. **72**, 2207 (1994).
[22] H. Tanaka, Phys. Rev. Lett. **70**, 53 (1993).
[23] H. Tanaka, Phys. Rev. Lett. **70**, 2770 (1993).
[24] P. Wiltzius, S. B. Dierker, and B. S. Dennis, Phys. Rev. Lett. **62**, 804 (1989).
[25] L. D. Gelb and K. E. Gubbins, Phys. Rev. E **55**, R1290 (1997).
[26] B. Strickland, G. Leptoukh, and C. Roland, J. Phys. A **28**, L403 (1995).
[27] B. K. Peterson, J. P. R. B. Walton, and K. E. Gubbins, J. Chem. Soc. Faraday Trans. 2 **82**, 1789 (1986).
[28] Z. Tan, F. van Swol, and K. E. Gubbins, Mol. Phys. **62**, 1213 (1987).
[29] B. K. Peterson, K. E. Gubbins, G. S. Heffelfinger, U. M. B. Marconi, and F. van Swol, J. Chem. Phys. **88**, 6487 (1988).
[30] M. P. Allen and D. J. Tildsley, *Computer Simulation of Liquids* (Clarendon Press, Oxford, 1987).
[31] D. A. Kofke and E. D. Glandt, Mol. Phys. **64**, 1105 (1988).
[32] E. de Miguel, E. M. del Rio, and M. M. T. de Gama, J. Chem. Phys. **103**, 6188 (1995).
[33] N. B. Wilding, Phys. Rev. E **52**, 602 (1995).
[34] B. A. Berg and T. Neuhaus, Phys. Rev. Lett. **68**, 9 (1992).
[35] C. Borgs and S. Kappler, Phys. Lett. A **171**, 37 (1992).
[36] L. D. Gelb and K. E. Gubbins, Physica A (to be published).
[37] S. Jiang and K. E. Gubbins, Mol. Phys. **86**, 599 (1995).
[38] K. K. Mon and K. Binder, J. Chem. Phys. **96**, 6989 (1992).
[39] W.-J. Ma, A. Maritan, J. R. Banavar, and J. Koplik, Phys. Rev. A **45**, R5347 (1992).
[40] M. Laradji, S. Toxvaerd, and O. G. Mouritsen, Phys. Rev. Lett. **77**, 2253 (1996).
[41] K. Binder, Z. Phys. B **43**, 119 (1981).
[42] H. Nakanishi and M. E. Fisher, J. Chem. Phys. **78**, 3279 (1983).